

Alpha-Particle Continuum States*

PAUL SZYDLIK†‡

Catholic University of America, Washington, D. C.

AND

CARL WERTZ

Catholic University of America, Washington, D. C. and U. S. Naval Ordnance Laboratory,
White Oak, Silver Spring, Maryland

(Received 4 January 1965)

The two-channel collision matrix for the $t+p \leftrightarrow {}^3\text{He}+n$ system is obtained by calculating the amplitudes for isotopic spin 0 and 1 for the scattering of a nucleon and an $A=3$ nucleus and combining these amplitudes in the proper linear combinations. The isotopic-spin amplitudes are obtained by making a resonating-group approximation for the continuum wave functions. It is found that with an "equivalent" central potential representing the nucleon-nucleon force the theory predicts the existence of two isotopic spin-0 *bound* excited states. These states, a 0^+ and a 1^- , are related to two experimentally observed structures in the cross sections. The good agreement of the theoretical and experimental cross sections in an energy region above the experimental peaks is used to establish the semiquantitative correctness of the pure isotopic-spin amplitudes obtained.

I. INTRODUCTION

IT is likely that the ${}^4\text{He}$ nucleus is the lightest nuclear system in which true resonances occur. At present, two broad resonances seem to be present in the $t+p$ and ${}^3\text{He}+n$ channels. They have been observed in both two-body scattering experiments and in reactions in which they are produced as parts of three-body final states.

The lower state, at an excitation of about 20.4 MeV, is observed most convincingly in the three-body-producing reactions $t(d,n)pt$ and ${}^3\text{He}(d,p)pt$.¹ The cross sections are strongly enhanced for those states in which the triton and proton come away with their relative energy in the neighborhood of 500 keV. A direct measurement by Jarmie² *et al.* of the 120° elastic $t+p$ cross section in the energy range including 500 keV has revealed a broad peak at about 300 keV which certainly corresponds to the structure produced in the breakup reactions. Wertz³ has shown that the results of both types of experiments can be understood in terms of an S -wave 0^+ resonance of the alpha particle at the excitation energy given above. Balashko and Kurepin⁴ come to the same conclusion from their analysis of their own $t+p$ data.

The more complete Brookhaven experiments of

Kane⁵ *et al.* also reveal a definite enhancement of the three-body breakup cross sections for relative energies in the $t+p$ and ${}^3\text{He}+n$ systems which correspond to an excitation energy of 22.2 MeV relative to the alpha ground state. This is also the energy at which broad peaks occur in the ${}^3\text{He}(n,n){}^3\text{He}$ ⁵ and $t(p,n){}^3\text{He}$ ⁶ total cross sections. Meyerhof⁷ has extended the single-pole approximation used in Ref. 3 to the energy region of the second peak in the breakup experiments and finds that it is due to strong p -wave interaction although none of his phase shifts go through 90° . The experimental two-body reactions require only $L=0, 1,$ and 2 terms in the Legendre polynomial expansions for the cross sections, and this would seemingly eliminate D and higher orbital-angular-momentum states as being involved. A group at Wisconsin⁸ has measured the polarization of the neutrons produced in the charge exchange $t+p$ reaction. The maximum polarization occurs at the energy of the second α peak, and the quantity $(d\sigma/d\Omega)P(\theta)$ has a $\sin\theta \cos\theta$ dependence. This distribution is consistent with a 1^- resonance in which spin-orbit coupling allows it to decay into either the spin-0 or spin-1 states.

The four-body system is still simple enough that one would like to understand its spectrum in terms of a basic nucleon-nucleon potential. We have undertaken a calculation using a purely central "equivalent" potential as a first step toward one which is based on a more complete nucleon-nucleon potential. However, we believe our calculations are reliable enough to indicate

* Work supported in part by U. S. Air Force Office of Scientific Research.

† NASA Predoctoral Fellow.

‡ Present address: University of California, Davis, California.

¹ H. W. Lefevre, R. R. Borchers, and C. H. Poppe, *Phys. Rev.* **128**, 1328 (1962); C. H. Poppe, C. H. Holbrow, and R. R. Borchers, *ibid.* **129**, 733 (1963); P. G. Young and G. G. Ohlsen, *Phys. Letters* **8**, 124 (1964); **11**, 192 (E) (1964); P. F. Donovan, J. V. Kane, J. F. Mollenauer, and P. D. Parker, *Bull. Am. Phys. Soc.* **9**, 389 (1964).

² Nelson Jarmie and Robert L. Allen, *Phys. Rev.* **114**, 176 (1959).

³ Carl Wertz, *Phys. Rev.* **128**, 1336 (1962); **133**, B19 (1964).

⁴ Yu G. Balashko and A. B. Kurepin, *Zh. Eksperim i Teor. Fiz.* **44**, 610 (1963) [English transl.: *Soviet Phys.—JETP* **17**, 414 (1963)].

⁵ J. D. Seagrave, L. Cranberg, and J. E. Simmons, *Phys. Rev.* **119**, 1981 (1960).

⁶ J. D. Seagrave, *Proceedings of the Conference on Nuclear Forces and the Few-Nucleon Problem, London 1959*, edited by T. C. Griffith and E. A. Power (Pergamon Press Ltd., London, 1960).

⁷ W. E. Meyerhof, *Conference on Correlations of Particles Emitted in Nuclear Reactions, Gatlinburg, 1964* (unpublished).

⁸ R. L. Walter, W. Benenson, P. S. Dobbeldam, and T. H. May, *Nucl. Phys.* **30**, 292 (1962).

the correct spin, parity, and isotopic-spin assignments to be given to the states.

Goldhammer⁹ has calculated the excitation energy of the first excited $T=1$ p state by employing the Feenberg-Bolsterli¹⁰ perturbation technique through second order. This calculation uses harmonic-oscillator wave functions as a basis and, thus, an infinite spectrum of discrete states is introduced into a system where only a few broad resonances occur. One cannot be certain that even two states shifted in energy by the perturbation correspond to any physical resonance. Under these circumstances it seems more reasonable to attempt to treat the problem directly as a scattering problem and calculate the two-channel scattering matrix for each partial wave.

Bransden, Robertson, and Swan¹¹ have calculated the cross sections for $t+n$ and ${}^3\text{He}+n$ elastic scattering by using the resonating-group method and have obtained remarkable agreement with experiment, particularly in the case of $t+n$ which is correctly considered as a one-channel scattering problem. In this method a cluster-type wave function is inserted into the Schrödinger equation and the best single-particle wave function for the fourth nucleon is found. The asymptotic values of the wave function are used to calculate the scattering phase shifts at any energy. Since the ${}^4\text{He}$ resonances are very broad they should be predominantly single particle and one might expect to represent them accurately by a resonating-group wave function.

Laskar¹² has formally derived coupled equations for the three-channel system $t+p \leftrightarrow {}^3\text{He}+n \leftrightarrow d+d$ which includes our two-channel system as a special case. However, he has numerical results only for the matrix elements U_{dd} , U_{pd} , and U_{nd} —none for the elements U_{pp} , U_{pn} , or U_{nn} in which we are primarily interested. The two-channel problem reduces to two single-channel ones—like those solved in Ref. 11—if the isotopic-spin invariance of nuclear forces is invoked. An $A=3$ nucleus and a nucleon can be coupled to a total isotopic spin of either 0 or 1. By analogy with pion-nucleon scattering one can calculate the pure isotopic-spin phase shifts and form the physically observed collision matrix elements by taking the proper linear combinations of the matrix elements for each isotopic spin state.

The justification for dealing with each isotopic spin state separately is that the coupling between the two states is small. The Coulomb potential which certainly couples the two states is two orders of magnitude less than the nucleon-nucleon potential. Brennan and Wertz¹³ have shown that the matrix element

$\langle T=1 | V_c | T=0 \rangle$ is $\cong 0.1$ MeV for the ${}^4\text{He}$ ground state so that the effective isotopic spin mixing potential is reduced by still another order of magnitude by the differing space symmetries of the two states. ($\langle T=0 | V_c | T=0 \rangle \cong 1.5$ MeV.)

In the calculations which are described below the interaction of the $A=3$ nucleus and a nucleon is considered for the four possible spin and isotopic spins and for $L=0, 1$, and 2. The calculated phase shifts show that there are two excited states, for purely central forces at least, and that these states are both $T=0$ with spin and parity 0^+ and 1^- . The two-channel scattering matrix is evaluated for a number of energies, and the excellent agreement of the calculated with the observed cross sections at energies above the observed resonances is used as evidence to support the assignments to the states.

II. COLLISION MATRIX

The region of excitation energies for which we intend to calculate the two-body cross sections is near the $t+p$ and ${}^3\text{He}+n$ thresholds. As a result, even though isotopic spin conservation obtains in the region of strong interaction the mass difference of the triton and ${}^3\text{He}$ and the presence of the long-range Coulomb force in the $t+p$ channel cause the matrix elements in the two channels to differ considerably. As an extreme example, only the matrix element U_{pp} exists physically for excitation energies below the threshold for ${}^3\text{He}+n$.

Before considering the problem in its full complexity it is perhaps instructive to review the calculation of the collision matrix elements in the absence of the electromagnetic interaction. Introducing the symbol h to represent the $A=3$ nucleus in its $T_z = +\frac{1}{2}$ state, the pure isotopic spin states can be written as linear combinations of the $t+p$ and ${}^3\text{He}+n$ states.

$$\begin{aligned} |T=0\rangle &= (1/\sqrt{2})(hn - tp), \\ |T=1\rangle &= (1/\sqrt{2})(hn + tp). \end{aligned} \quad (1)$$

In the absence of a nuclear interaction between pairs an expansion of hn (or tp) in terms of the pure isotopic spin states,

$$hn = (1/\sqrt{2})(|T=0\rangle + |T=1\rangle), \quad (2)$$

has the meaning that only a noninteracting ${}^3\text{He}+n$ pair is present. In the presence of an interaction the same equation now represents a plane ${}^3\text{He}+n$ wave plus outgoing ${}^3\text{He}+n$ and $t+p$. For a given angular momentum and parity channel the above considerations lead to the following expressions for the collision matrices appropriate to the processes ${}^3\text{He}(n,n){}^3\text{He}$, ${}^3\text{He}(n,p)t$, $t(p,n){}^3\text{He}$, and $t(p,p)t$:

$$\begin{aligned} U_{nn} &= \frac{1}{2}[U(0) + U(1)], \\ U_{pn} = U_{np} &= \frac{1}{2}[U(0) - U(1)], \\ U_{pp} &= \frac{1}{2}[U(0) + U(1)]. \end{aligned} \quad (3)$$

⁹ Paul Goldhammer, thesis, Washington University, St. Louis, 1956 (unpublished).

¹⁰ Mark Bolsterli and Eugene Feenberg, Phys. Rev. **101**, 1349 (1956).

¹¹ B. H. Bransden, H. H. Robertson, and P. Swan, Proc. Phys. Soc. (London) **69A**, 60 (1956).

¹² William Laskar, Ann. Phys. (N. Y.) **17**, 436 (1962).

¹³ J. G. Brennan and Carl Wertz, Phys. Letters **6**, 113 (1963).

The quantity $U(T)$ is the pure isotopic spin-matrix element.

Baž¹⁴ has shown how the above equations can be modified to take into account the Coulomb effects. One assumes that there is an interaction radius a beyond which there are no nuclear forces. At this radius the logarithmic derivative of a pure isotopic spin state is taken to be the same in either the ${}^3\text{He}+n$ or $t+p$ channels. Denoting these derivatives by $L(T)$ and introducing the appropriate asymptotic wave functions for the two channels, two new "pure" isotopic-spin matrix elements can be obtained which contain the effects due to the difference of the thresholds and the long-range effect of the Coulomb force,

$$S(T) = \frac{-k_n n_L' + L(T) n_L - i(k_n j_L' - L(T) j_L)}{\text{complex conjugate}} \Big|_{\rho=ka}, \quad (4)$$

$$\Omega(T) = \frac{k_p G_L' - L(T) G_L - i(k_p F_L' - L(T) F_L)}{\text{complex conjugate}} \Big|_{\rho=kpa}.$$

In the above equation the prime denotes differentiation of a function with respect to its argument. The regular and irregular channel functions have their usual definitions. The c.m. wave numbers of the two channels are related by $\hbar^2 k_n^2 = \hbar^2 k_p^2 - 2(3m/4)E_t$. The energy E_t is the threshold energy in the $t+p$ c.m. system and is numerically ≈ 0.76 MeV.

The collision matrix elements can be shown to be related to $S(T)$ and $\Omega(T)$ by the equations

$$U_{nn} = \frac{\gamma_{22}[S(0)+S(1)] - \gamma_{12}[\Omega(0)S(0) + \Omega(1)S(1)]}{2\gamma_{22} - \gamma_{12}[\Omega(0) + \Omega(1)]},$$

$$U_{pn} = U_{np} = (k_n/k_p)^{1/2} \frac{S(0) - S(1)}{2\gamma_{12} + \gamma_{12}[S(0) + S(1)]}, \quad (5)$$

$$U_{pp} = \frac{\gamma_{11}[\Omega(0) + \Omega(1)] + \gamma_{12}[\Omega(0)S(0) + \Omega(1)S(1)]}{2\gamma_{11} + \gamma_{12}[S(0) + S(1)]}.$$

The hitherto undefined quantities γ_{ij} depend on the channel functions and their derivatives evaluated at the nuclear surface. Their definition can be found in Appendix A. We note that in the limit of large E_p/E_t , $\gamma_{12} \rightarrow 0$, $S(T) \rightarrow \Omega(T)$, and the expressions in Eq. (5) reduce to those of Eq. (3).

For completeness we define the differential cross sections in terms of the collision matrix elements. Since central forces are being used throughout the calculation the total spin and the orbital angular momentum in a channel are good quantum numbers. Then the matrix element in a given partial wave can be represented by $U_{ij}(sL)$. The usual expressions obtain for the cross

sections,

$$\frac{d\sigma_{ij}}{d\Omega} = \frac{1}{4} |f_{ij}^0(\theta)|^2 + \frac{3}{4} |f_{ij}^1(\theta)|^2, \quad (6)$$

where, except for $i=j=p$, the amplitudes f_{ij}^s are given by

$$f_{ij}^s(\theta) = \frac{1}{k_i} \sum (2L+1) \frac{[U_{ji}(sL) - \delta_{ij}]}{2i} P_L(\cos\theta). \quad (7a)$$

For elastic scattering in the charged channel the amplitudes are

$$f_{pp}^s(\theta) = f_c(\theta) + \frac{1}{k_p} \sum_L (2L+1) (\exp - 2i\omega_L) \times \frac{[U_{pp}(sL) - 1]}{2i} P_L(\cos\theta), \quad (7b)$$

$$f_c(\theta) = -(1/2k)\eta \csc^2(\theta/2) \times \exp[-2i\eta \ln \sin(\theta/2)].$$

The Coulomb phase shift $\omega_L = \sigma_L - \sigma_0$ appears because of the way in which the spherical Coulomb waves have been defined. (See Appendix A.)

III. INTERNAL WAVE FUNCTIONS

The formulas of the preceding section give the dependence of the scattering matrix on the logarithmic derivatives of the channel wave functions evaluated at some radius larger than the radius of interaction. We give below a discussion of the approximation to the Schrödinger equation we have used in order to obtain internal wave functions, and hence, the required logarithmic derivatives. This approximation, the resonating group approximation,^{11,15,16} has been used extensively in treating theoretically the scattering of light nuclei.

Suppose one wants to consider the elastic scattering of a system A from a system B . The total Hamiltonian can be written as the sum representing the internal motions of A and B and a term consisting of the kinetic energy of relative motion and the sum of the two-body potentials acting between pairs of nucleons which are split between the two nuclei A and B . The Schrödinger equation is written as

$$\{H_A - H_B - (\hbar^2/2\mu)\nabla^2 + \sum_{\substack{i \in A \\ j \in B}} V_{ij} - E\} \Psi = 0. \quad (8)$$

The resonating group approximation consists in writing the solution as the antisymmetrized product of the internal wave functions for A and B and a function of the

¹⁴ A. I. Baž, Zh. Eksperim. i Teor. Fiz. 32, 478 (1957) [English transl.: Soviet Phys.—JETP 5, 403 (1957)].

¹⁵ J. A. Wheeler, Phys. Rev. 52, 1107 (1937).

¹⁶ Y. C. Tang, E. Schmid, and Karl Wildermuth, Phys. Rev. 131, 2631 (1963).

relative coordinate of the centers of A and B ;

$$\Psi = \sum (-1)^P P \Psi_A \Psi_B \Phi(\mathbf{r}_A - \mathbf{r}_B). \quad (9)$$

Upon inserting this function into the Schrödinger equation, multiplying from the left by $\Psi_A^* \Psi_B^*$, and integrating over the internal coordinates of A and B , one obtains an integrodifferential equation for $\Phi(\mathbf{r})$.

$$[-\nabla^2 + U(r) - k^2] \Phi(\mathbf{r}) = - \int d\mathbf{r}' K(\mathbf{r}, \mathbf{r}') \Phi(\mathbf{r}'), \quad (10)$$

$$k^2 = \frac{2\mu}{\hbar^2} [E - \langle \Psi_A | H_A | \Psi_A \rangle - \langle \Psi_B | H_B | \Psi_B \rangle].$$

For large $|\mathbf{r}|$ the equation takes the form

$$[-\nabla^2 + k^2] \Phi(\mathbf{r}) = 0, \quad (11)$$

which shows that the approximate solution has the correct form in the asymptotic region. The kernel $K(\mathbf{r}, \mathbf{r}')$ arises from the exchange terms and is explicitly a function of the total energy E . This has the consequence that a set of solutions obtained by imposing boundary conditions on the surface of a finite volume are not, in general, orthogonal. However, the set of properly antisymmetrized functions formed from the $\Phi(\mathbf{r})$'s are orthogonal.

Equation (10) can also be obtained from a variational principle

$$\delta \int \Psi^* (H - E) \Psi = 0, \quad (12)$$

in which the variation is taken with respect to $\Phi(\mathbf{r})$ alone and the total energy as defined in Eq. (10) is held fixed. Since the true solution obeys the same variational principle with no restriction as to the variation of Ψ it follows that if the true solution is nearly of the resonating group form we get a very good solution to the problem. Conversely, if we have a poor approximation in the beginning, the resonating group method can give a very poor result.

Since Eq. (12) is a variational principle and not a minimal principle it is clear that for $k^2 > 0$ one can not say *a priori* whether a calculated phase shift is greater or less than that corresponding to the correct solution. However, it may happen that there are exponentially decaying solutions to Eq. (10) for certain $k^2 < 0$. That solution which approximates the ground state of the system in a given channel of A and B is a trial wave function in the sense of the Rayleigh-Ritz principle and $E_0(k^2)$ is an upper bound on the actual ground-state energy. That this is true follows from the observation that the best trial wave function of a given type, that is, the one with the lowest energy, satisfies the variational equation

$$\delta \int \Psi_i^* (H - E_i) \Psi_i = 0, \quad (13)$$

$$\delta E_i = 0.$$

Since δE_i is given by

$$\delta E_i = (2 \operatorname{Re} \langle \Psi_i | H - E_i | \delta \Psi_i \rangle) / \langle \Psi_i | \Psi_i \rangle, \quad (14)$$

it is clear that a solution to Eq. (10) is the product function which gives the lowest energy. [We note that $\langle \Psi | \Psi \rangle$ exists only for decaying exponential solutions so that solutions to Eq. (10) with lower energy have no physical significance.]

If there is a solution to the resonating-group equation for a second $k^2 < 0$ in a given channel of A and B , $E_1(k_1^2)$ is no longer an upper bound to the energy of the first excited state because there can still be some admixture of the true ground state into the excited state. However, if $\langle \Psi_1 | \Psi_0 \rangle$ is small one may hope that the estimate of the energy is accurate. Actually, both situations occur in the calculation under discussion. We obtain a total energy for the 1P_1 state which is lower than the total energy of the $A=3$ cluster plus nucleon so that this energy is an upper bound to the energy of the state. The 1S_0 state also turns out to be slightly bound, but since the ground state of the alpha particle has the same quantum numbers the calculated energy is not an upper bound to the actual energy of the state.

In the present calculation the four-body wave function is constructed from the product of an $S = \frac{1}{2}$, $T = \frac{1}{2}$ cluster representing the $A=3$ nucleus and a single $S = \frac{1}{2}$, $T = \frac{1}{2}$ nucleon. With central forces the ground state of the three-body system is an S state. However, the differing magnitudes of the singlet and triplet forces causes mixed symmetry and antisymmetric S state to be mixed into the predominantly space-symmetric ground state. The latest calculations by Blatt and Delves¹⁷ indicate that with the most complete nucleon-nucleon potentials this admixture is the order of about 1%. Since for our "equivalent" central potential the relevant quantity $V_i^+(\mathbf{r}) - V_s^+(\mathbf{r})$ is roughly of the same size as the $V_s^+(\mathbf{r}) - V_i^+(\mathbf{r})$, the difference between the central-singlet and central-triplet part of a complete potential, we are safe in taking the ground state to be totally space symmetric. Thus, the four-body resonating-group wave function for a given spin S , isotopic spin T , and orbital angular momentum L can be written as

$$\Psi_L^{ST}(1234) = \sum_P (-1)^P \Psi([\bar{1}23])$$

$$\times (f_L^{ST}(r_4)/r_4) P_L(\cos\theta_4)$$

$$\times \sum_{m'} (\frac{1}{2} S; m', m - m', m)$$

$$\times \chi^{m'}(\{12\}, 3) \chi^{m-m'}(4)$$

$$\times \sum_{t'} (\frac{1}{2} T; t', t - t', t)$$

$$\times \eta^{t'}([\bar{1}2], 3) \eta^{t-t'}(4), \quad (15)$$

¹⁷ J. M. Blatt and L. M. Delves, Phys. Rev. Letters **12**, 544 (1964).

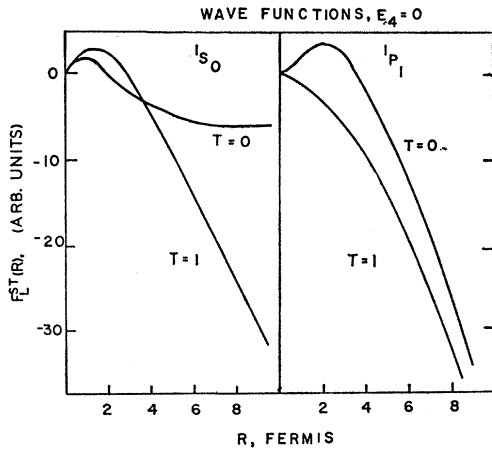


FIG. 1. The wave function $f_L^{ST}(r)$ plotted as a function of r for selected values of L, S , and T . The normalizations are arbitrary.

where $[ij\cdots]$ denotes a function symmetric in the indices and $\{ij\}$ denotes a function antisymmetric in the indices. The space function Ψ is that of the three-body cluster while χ^m and η^t are mixed-symmetry spin and isospin functions.

In order to facilitate the integrations a Gaussian form was chosen for both the three-body cluster, represented by

$$\Psi([123]) = N^{1/2} \exp(-\mu \sum_{i,j} r_{ij}^2), \quad (16)$$

and the two-body potentials,

$$V_{s,t^+}(r) = -V_{s,t} \exp(-\lambda r^2). \quad (17)$$

The parameter μ was chosen so that the rms radius of the three-body cluster is equal to 1.69 F, a value consistent with the rms radius of the space-symmetric part of the three-body cluster obtained from electron scattering.¹⁸ The parameters of the nucleon-nucleon potential are taken from the work of Tang *et al.*¹⁶ The values of the parameters are

$$\begin{aligned} \mu &= 0.05905 \text{ F}^{-2}, & \lambda &= 0.46 \text{ F}^{-2}, \\ V_s &= 45.98 \text{ MeV}, & V_t &= 72.98 \text{ MeV}. \end{aligned} \quad (18)$$

It is worthwhile to note at this point that there are no more free parameters in the theory.

The wave function of Eq. (15) leads to the following integrodifferential equation for the fourth particle function $f_L^{ST}(r)$;

$$\begin{aligned} \left[\frac{-d^2}{dr^2} + \frac{L(L+1)}{r^2} + U^{ST}(r) - k^2 \right] f_L^{ST}(r) \\ = - \int_0^\infty dr' K_L^{ST}(r,r') f_L^{ST}(r'). \end{aligned} \quad (19)$$

¹⁸ L. I. Schiff, Phys. Rev. **133**, B802 (1964); B. K. Srivastava, *ibid.* **133**, B545 (1964).

The explicit forms for the direct potential $U^{ST}(r)$ and the kernel $K_L^{ST}(r,r')$ are listed in Appendix B. The equations were solved numerically on the Naval Ordnance Laboratory IBM-7090 following the procedure outlined by Robertson.¹⁹ In the final "runs" a mesh containing 34 points, spaced 0.3 apart, was used. This allowed us to evaluate the single-particle wave function out to 9.9 F which is about 2 F larger than the practical limit of the nuclear forces. This radius is also sufficiently large that for $k^2 > 0$, the kernel term contributes effectively zero. Unfortunately, this is not the case for $k^2 < 0$ since the function blows up exponentially for larger $|r|$. Without rewriting our program to allow us to take more mesh points, we can only infer the positions of ground states from the behavior of the phase shifts.

Note that the Coulomb potential does not appear in either term because we are treating it as a perturbation of the forces.

IV. NUMERICAL RESULTS

Equation (18) has been solved for the set of states $L=0, 1, 2, S=0, 1, T=0, 1$. Several representative functions $f_L^{ST}(r)$ are plotted in Fig. 1. They are all solutions for zero relative energy, that is $k^2=0$. It is apparent from the positive slope for large r of the ${}^1S_0, T=0$ function that in this model there is a second bound S state of the alpha particle just below the threshold for two-body breakup. The node in the ${}^1P_1, T=0$ function means that there is also a bound P state several MeV below the threshold. It can be shown that the phase shifts which are obtained from solving the resonating group equations satisfy modified effective-range expansions so we have estimated the energies of the bound states by finding the negative energy poles of the effective-range expansion for the scattering amplitudes. The

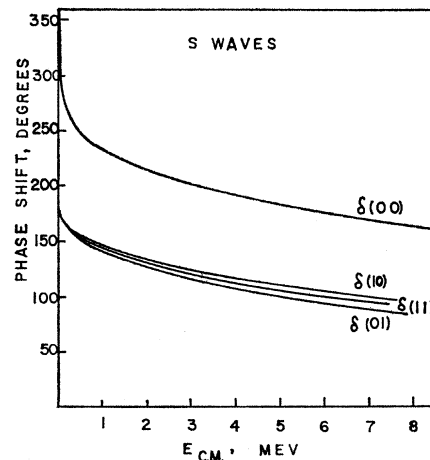


FIG. 2. S -wave phase shifts $\delta(ST)$ as a function of the relative energy of the fourth nucleon and the $A=3$ core. The Coulomb force has been neglected.

¹⁹ H. H. Robertson, Proc. Cambridge Phil. Soc. **52**, 538 (1956).

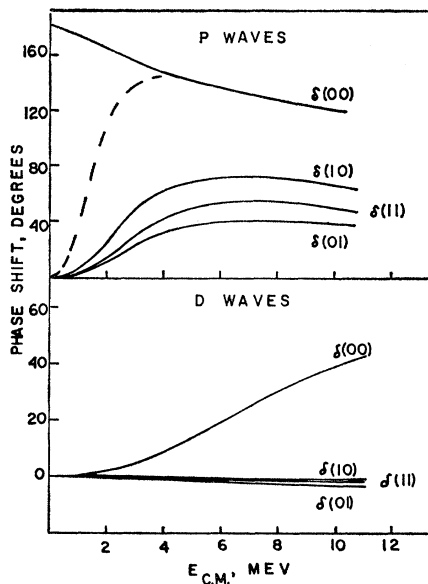


FIG. 3. P - and D -wave phase shifts $\delta(ST)$ as a function of the energy of the fourth nucleon and the $A=3$ core. The Coulomb force has been neglected. The dashed line represents a possible energy dependence of the $T=0$, 1P_1 phase shift if the state is moved from below the threshold into the continuum region. The resulting total cross sections are compared with the data in Figs. 8 and 9.

estimated energies, relative to the two-body threshold, are

$$\begin{aligned} {}^1S_0: E &\cong -290 \text{ eV}; \\ {}^1P_1: E &\cong -2.7 \text{ MeV}. \end{aligned} \quad (20)$$

The 3S_1 , $T=0$ function is typical of the other three S states. In spite of the absence of a bound state the function has a node in it. This comes about because of the Pauli principle which forbids a third neutron from being in a $1s$ state. The phase shift starts at π and decreases essentially like a hard-sphere phase shift. This is an example of a theorem discussed by Swan.²⁰ The phase shift at zero energy for scattering from a composite system approaches $(n+m)\pi$, where n is the number of bound states and m is the number of states excluded by the Pauli principle. In the 3S_1 case, $n=0$ and $m=1$ while for the 1P_1 state $n=1$, $m=0$. Finally, the 1P_1 , $T=1$ state is added to show what a typical non-resonant P state looks like.

Since the Coulomb force has been neglected, the wave function in a given L , S , and T channel for large $|\mathbf{r}|$ takes the form

$$f_L^{ST}(r) \propto j_L(kr) - \tan \delta_L n_L(kr), \quad (21)$$

where δ_L is real. An examination of the $k^2=0$ S -wave functions shows that the wave functions become straight lines for $r \geq 8.1$ F. This radius was used for all states as the radius at which the logarithmic derivatives

$L(T)$ of the inside functions were evaluated. The sets of $L(T)$ determine the scattering cross sections as outlined in Sec. II and they can also be used to calculate the "pure" isotopic spin phase shifts defined in Eq. (21). The phase shifts so obtained are displayed in Figs. 2 and 3.

It is interesting to note that only in the $S=0$, $T=0$ states are the forces attractive for all L values. The contributions of the exchange integral are generally of one sign for even-parity states and of the opposite for odd ones. In the spin-isospin singlet state the attractive direct potential dominates and the over-all forces are always attractive. In the other three spin-isospin states the kernel dominates for low L values and in the even-parity states the phase shifts reflect the over-all repulsion.

The total ${}^3\text{He}(n,n){}^3\text{He}$ and $t(p,n){}^3\text{He}$ cross sections have been calculated and are compared with the experimental^{21,5,6} values in Figs. 4 and 5. The fit at the higher energies is excellent but very poor at the lower ones. This also is reflected in the angular distributions of the $t(p,p)t$, $t(p,n){}^3\text{He}$, and ${}^3\text{He}(n,n){}^3\text{He}$ reactions. In Fig. 6 the theoretical and experimental^{6,21,22} differential cross sections are compared for a c.m. energy $E_p=6.0$ MeV. The fit is astoundingly good, whereas, as shown in Fig. 7 the fit is very poor at $E_p(\text{c.m.})=2.25$ MeV, the energy of the peak in the $t(p,n){}^3\text{He}$ total cross section.

It should be noted before we discuss the significance of the results that the logarithmic derivatives $L(T)$ are evaluated for an energy E related to the observed energies by $E=E_p-E_{\text{Coul}}$, where E_{Coul} is the Coulomb energy of the internal state. This energy varies from state to state but is always of the order of 0.5 MeV.

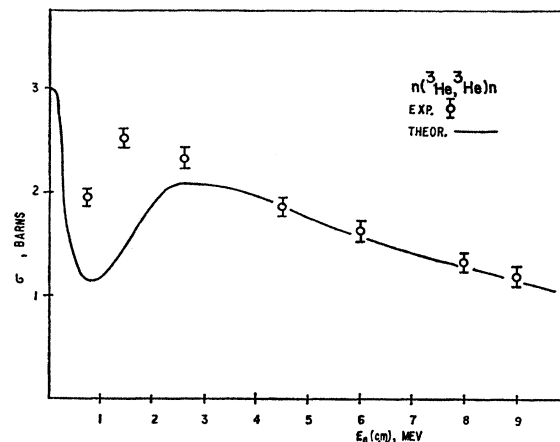


FIG. 4. A comparison of the calculated and observed total elastic-neutron cross section. The data points are taken from Ref. 5.

²¹ W. E. Wilson, R. L. Walter, and D. B. Fossan, Nucl. Phys. 27, 421 (1963).

²² R. A. Claassen, J. S. Brown, G. D. Freier, and W. R. Stratton, Phys. Rev. 82, 593 (1951); J. E. Brolley, Jr., T. M. Putnam, L. Rosen, and L. Stewart, *ibid.* 117, 1307 (1960).

²⁰ K. B. Mather and P. Swan, *Nuclear Scattering* (Cambridge University Press, Cambridge, England, 1958), Appendix 13.

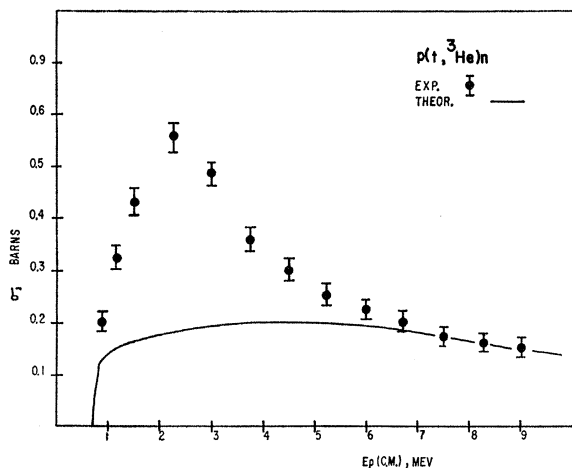


FIG. 5. A comparison of the calculated and observed total pn cross section. The data points are a sample of points found in Refs. 6 and 21.

One numerical result which is of interest is a set of values for the two $n+t$ scattering lengths. They are

$$\begin{aligned} \text{singlet: } a_s &= 3.38 \text{ F,} \\ \text{triplet: } a_t &= 3.25 \text{ F.} \end{aligned} \quad (22)$$

These values yield a thermal-neutron cross section of $\sigma = 1.35 \text{ b}$ which is consistent with the extrapolated value from the Los Alamos data.²³

It has been brought to our attention²⁴ that it is experimentally possible to measure separately the singlet and triplet thermal-neutron cross sections for the process ${}^3\text{He}(n,p)t$. For small k_n, k_p an S -wave transition matrix element T can be written in terms of a complex scattering length A :

$$T = k_p^{1/2} k_n^{1/2} A. \quad (23)$$

We have computed the cross sections for both spin states at 6 keV and have obtained values for the singlet and triplet inelastic scattering lengths. They are

$$\begin{aligned} A_s &= 4.44 + i(5.15) \text{ F,} \\ A_t &= 0.087 - i(0.045) \text{ F.} \end{aligned} \quad (24)$$

The corresponding contributions to the cross section for unpolarized thermal neutrons onto an unpolarized target are

$$\begin{aligned} \pi k_p/k_n |A_s|^2 &= 8030 \text{ b,} \\ 3\pi k_p/k_n |A_t|^2 &= 5 \text{ b.} \end{aligned} \quad (25)$$

The observed value for the sum of the two is 5280 b so that our value is about 60% too high. The reason is that the energy of the "pure" isotopic spin state calculated from our model $\cong 0 \text{ keV}$ while the estimated¹³ energy of the pure state corresponding to the physical state seen in $t-p$ scattering $\cong -150 \text{ keV}$. In fact, the

²³ Los Alamos Physics and Cryogenics Group, Nucl. Phys. **12**, 291 (1959).

²⁴ L. Passell and R. I. Schirmer (private communication).

singlet $t-p$ phase shift calculated from our model only reaches $\sim 65^\circ$ at the ${}^3\text{He}+n$ threshold; the resonance is, in effect, shifted upwards several hundred keV from its observed value. (Strictly speaking, instead of a true resonance we have a *virtual state*.)

The small contribution of the triplet state to the cross section arises from the near equality of the isotopic spin-0 and -1 amplitudes in the triplet state. In each case the effect of the Pauli principle is to produce phase shifts that are nearly hard sphere. The scattering am-

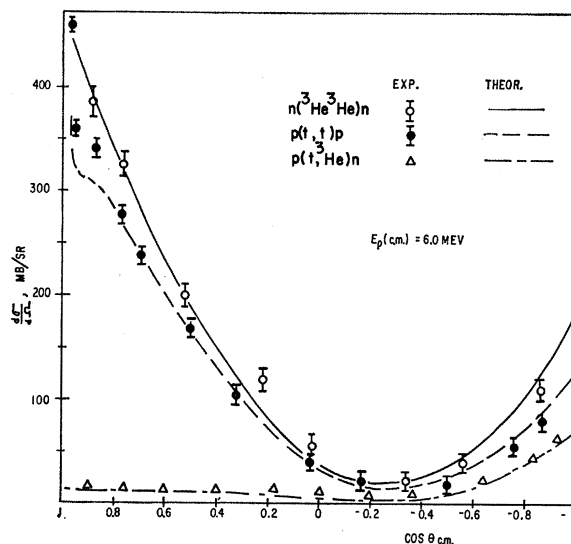


FIG. 6. A comparison of the calculated and observed differential cross sections for all modes of the two-channel scattering at a center-of-mass energy of 6.0 MeV in the $t+p$ channel. The data points for the nn reaction were obtained from Ref. 5, those for pp from Ref. 22, and the pn from Ref. 21. In all cases the points for the nearest experimental energy to 6.0 MeV were used.

plitude for the charge exchange reaction is essentially the difference of the pure isotopic-spin amplitudes, so it is very small in the triplet state. Since the 5-b value quoted above is obtained by taking the difference of two quantities which are only approximately determined it should be taken as an order-of-magnitude estimate.

V. DISCUSSION

In gauging the significance of our calculation there are essentially two points to be considered. The first point concerns the accuracy of our solutions to the purely mathematical problem of determining the scattering phase shifts for a given potential. In other words, given our simplified "equivalent" potential how closely do the resonating-group wave functions approximate the true solutions? The second point involves the question of how well the "equivalent" potential represents the vastly more complicated two-nucleon potentials derived from the study of nucleon-nucleon scattering.

There exist calculations which give some answers to

these questions. For example, Humberston²⁵ has used an equivalent central potential in calculating the doublet and quartet $n-d$ scattering lengths. The resonating-group solutions give values for the scattering lengths that are very near to one experimental set:

$$\begin{aligned} a_2 &= +0.7 \text{ F}, \\ a_4 &= +6.38 \text{ F}. \end{aligned} \quad (26)$$

However, he gets a better estimate by making use of a variational principle²⁶ that gives an upper bound on the scattering lengths. He finds that by introducing polarization of the deuteron the upper limit on a_2 is reduced well below the experimental value while a_4 remains appreciably unchanged. The implications of this calculation are twofold. For a given potential the resonating-group method may give a poor result in a channel that contains a bound state; an equivalent potential is at best a semiquantitative approximation to the complete nucleon-nucleon potential. On the other hand, for those states in which the Pauli exclusion principle acts to make the interaction essentially hard sphere the resonating-group approximation + an equivalent potential should give reliable results.

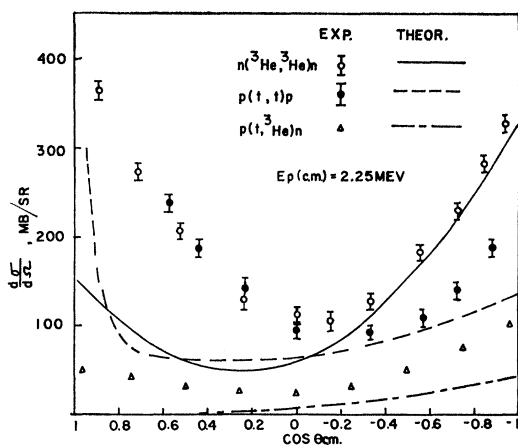


FIG. 7. A comparison of the calculated and observed differential cross sections for all modes of the two-channel scattering at a center-of-mass energy of 2.25 MeV in the $t+p$ system. The pp data were taken from Ref. 22, the nn from Ref. 5, and the pn from Ref. 6.

It should be noted that we have attempted to solve the problem in a way which does some violence to the mathematical consistency of the approximation but may improve the validity of the results. It will be recalled that the size of the three-body cluster has adjusted so that the rms radius is consistent with the radius observed in electron scattering from ^3He and ^3H . The three-body energy inserted into Eq. (19) is the

energy appropriate to this radius. However, the minimum energy of the three-body cluster occurs for a smaller radius and the value of the energy is appreciably lower. The radii and energies are listed below:

$$\begin{aligned} \bar{r} &= 1.69 \text{ F}, & E_3 &= -4.125 \text{ MeV}, \\ \bar{r} &= 1.20 \text{ F}, & E_3 &= -7.149 \text{ MeV}. \end{aligned} \quad (27)$$

The argument which we use in favor of our choice is that the resonating-group approximation consists in assuming that the incoming nucleon scatters off a nucleon distribution in the target nucleus that is undistorted by the incoming nucleon. The scattering from each of the target nucleons is represented tolerably well by the equivalent potential so that by introducing the correct nucleon spacing in the target nucleus one applies, perhaps, the approximation most realistically.

Our discussion concludes with the association of the two calculated states with structures seen in the experimental cross sections. Our 0^+ , $T=0$ state certainly corresponds to the peak observed in low-energy $t+p$ scattering. The calculated energy is of the order of 150 keV larger than the observed energy. The over-all interaction is repulsive in the other three S states so that the correspondence is unambiguous. The situation is less clear in regard to the 1^- , $T=0$ state because of the large discrepancy in the energies. However, we feel that the excellent agreement of our calculated cross sections and the observed ones at the higher energies makes the assignment of the quantum numbers 1^- , $T=0$ to the alpha resonance at 22.2 MeV very reasonable. In particular, the large backward peaking in the $t(p,n)^3\text{He}$ angular distributions at the higher energies arises from an interference of the 1D_2 , $T=0$ amplitude with the 1P_1 , $T=0$ amplitude. The sign of the interference is that corresponding to the 1P_1 phase shift being between $\frac{1}{2}\pi$ and π and the 1D_2 phase shift being between 0 and $\frac{1}{2}\pi$.

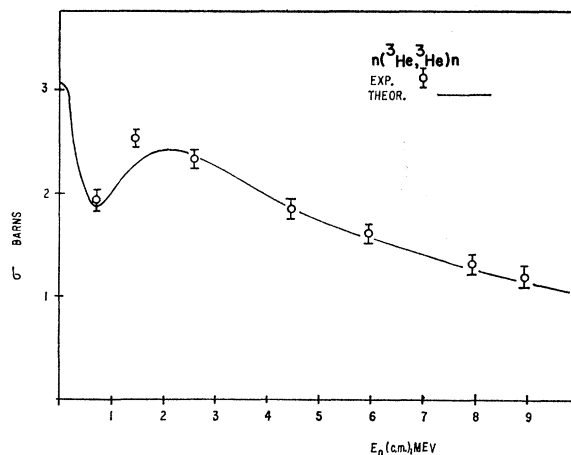


FIG. 8. A comparison of the total nn cross section calculated by assuming a broad $T=0$, 1^- resonance at about $E_p(\text{c.m.})=2.25$ MeV and the experimental values in Ref. 5. No other phase shifts have been changed from those values used to calculate the curve in Fig. 4.

²⁵ John Humberston, thesis, University College, London, 1964 (unpublished).

²⁶ Y. Hahn, T. F. O'Malley, and L. Spruch, Phys. Rev. 130, 381 (1963).

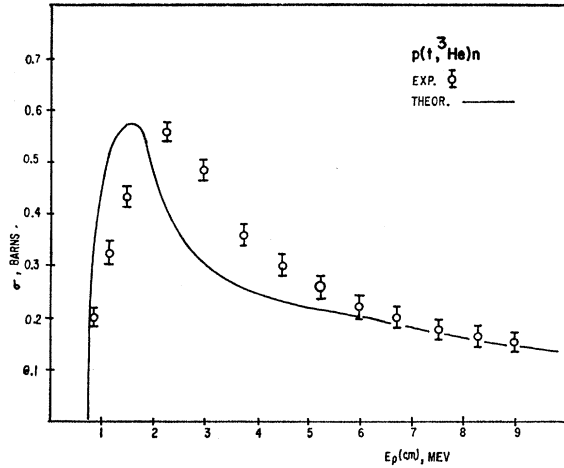


FIG. 9. A comparison of the pn total cross section calculated by assuming a broad $T=0, 1^-$ resonance at about $E_p(\text{c.m.})=2.25$ MeV and the experimental points of Refs. 6 and 21. No other phase shifts have been changed from those values used to calculate the curve in Fig. 5.

A check was made on these conjectures by putting into the calculation of the cross sections logarithmic derivatives in the $T=0, 1S_0$ and $1P_1$ channels corresponding to resonances at roughly the observed energies. A remainder term R , was included so that

$$a[L(T)] = \frac{E_\lambda - E}{\gamma^2 - (E_\lambda - E)R} + B, \quad (28)$$

$$a = 8.1F, \quad \gamma^2 = 1 \text{ MeV},$$

$$E = E_p - E_{\text{Coul}},$$

the derivatives equaled the ones originally calculated at $E_p \geq 4.50$ MeV. The constants B were chosen such that

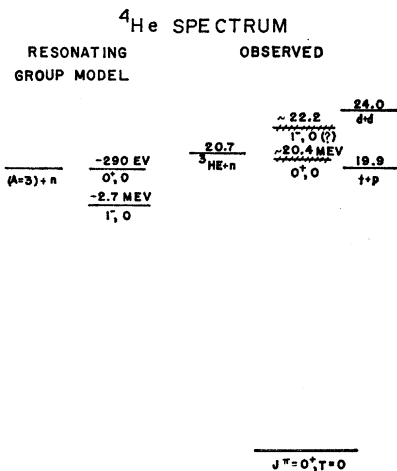


FIG. 10. The energy states of a nucleon scattering from a three-nucleon cluster calculated using an equivalent central potential and the proposed energy spectrum of the ^4He nucleus. The size of the three-nucleon cluster and the parameters of the two-nucleon potential are given in Eqs. (29) and (18) of the text.

the logarithmic derivatives were equal, respectively, to G_0'/G_0 at $E_p=0.5$ MeV and to G_1'/G_1 at $E_p=2.2$ MeV. No other phase shifts were changed from their previously calculated values. That an immense improvement was made in the total cross sections can be seen in Figs. 8 and 9. No attempt to improve the fit was made since our program for calculating the cross sections from the logarithmic derivatives does not at present contain provisions for including spin-flip terms, spin-orbit splitting, and other couplings allowed by the complete nucleon-nucleon potential.

In conclusion, we have plotted in Fig. 10 the calculated energy spectrum for ^4He obtained in this calculation and the proposed energy spectrum deduced from observation with the help of our calculation.

ACKNOWLEDGMENTS

We wish to thank Professor Brennan of Catholic University for help with the preliminary steps in our calculation as well as for his helpful comments in the later stages. We also thank Dr. Simons and Mrs. Susan Madigosky of the Naval Ordnance Laboratory for their constant help in facilitating our use of the IBM-7090 computer at the laboratory. One of us (P.S.) was aided in the earlier period of his graduate training by being the holder of an Atomic Energy Commission Fellowship.

APPENDIX A

In his derivation of the dependence of the two-channel U matrix on the logarithmic derivatives of the pure isotopic spin states BaZ^{14} has introduced the following asymptotic radial wave functions for the neutron and proton channels;

$$R_{nL}^\pm = k_n[-n_L(k_n r) \pm i j_L(k_n r)], \quad (A1)$$

$$R_{pL}^\pm = (1/r)[G_L(k_p r) \pm i F_L(k_p r)].$$

In the energy region below the $^3\text{He}+n$ threshold but above the threshold for $t+p$ the neutron channel wave functions are obtained from the expression above by making the substitution $k_n \rightarrow iK_n$. The quantities γ_{ij} which appear in Eq. (5) are combinations of the above radial functions evaluated at the nuclear surface. They are

$$\gamma_{11} = \gamma_{22}^* = - (a^2/2ik_p) \times [R_{nL}^- R_{pL}^+ - R_{nL}^+ R_{pL}^-] |_a, \quad (A2)$$

$$\gamma_{12} = \gamma_{21}^* = (a^2/2ik_p) [R_{nL}^+ R_{pL}^+ - R_{nL}^- R_{pL}^-] |_a.$$

Once again the correct form for $E_n < 0$ can be obtained by making an analytic continuation to the region where $k_n = iK_n$.

APPENDIX B

In this calculation we have restricted ourselves to an "equivalent" central Serber potential which in this

TABLE I. Coefficients of terms in Eq. (B2) for a central Serber potential. The strength of the singlet (triplet) potential is given by $-V_1$ ($-V_3$).

| | $S=0$ | | $S=1$ | |
|----------|---------------|---------------|---------------|--------------|
| | $T=0$ | $T=1$ | $T=0$ | $T=1$ |
| α | $-3(V_1+V_3)$ | $-2V_1$ | $-2V_3$ | $-(V_1+V_3)$ |
| β | $-3(V_1+V_3)$ | $+2V_1$ | $+2V_3$ | $+(V_1+V_3)$ |
| γ | $-3(V_1+V_3)$ | $-2V_1$ | $-2V_3$ | $-(V_1+V_3)$ |
| δ | $-3(V_1+V_3)$ | $-(V_1-3V_3)$ | $-(V_3-3V_1)$ | $+(V_1+V_3)$ |
| η | $+3$ | -1 | -1 | -1 |

section is written

$$V(r) = -V_{1,3} \exp(-\lambda r^2), \quad (\text{B1})$$

where $-V_1$ and $-V_3$ are the respective singlet and triplet strengths. The steps in obtaining explicit expressions for the direct potential $U(r)$ and the kernel $K(r, r')$ which appear in the integrodifferential Eq. (19) can be found in Ref. 11. In fact, those for $T=1$ are exactly the same as the direct potential and the kernel listed in this reference for $n+i$ scattering. We wish to catalog in this appendix the explicit expressions for both values of the isotopic spin, and for convenience we adopt essentially the same notation as Bransden, Robertson, and Swan. Equation (19) is written in a slightly altered form as

$$\begin{aligned} & (+2\hbar^2/3m) [-d^2/dr^2 + L(L+1)/r^2 - k^2] f_L(r) \\ & = -\alpha U(r) f_L(r) - \int dr' K_L(r, r') f_L(r'), \quad (\text{B2}) \end{aligned}$$

where the spin and isotopic-spin indices have been suppressed. The coefficient α depends on S and T and its values are listed in Table I. The kernel can also be expanded into a sum of terms whose coefficients depend on S and T ;

$$\begin{aligned} K_L(r, r') = & \beta [q_L(r, r') + s_L(r, r')] \\ & + \gamma t_L(r, r') + \delta r_L(r, r') \\ & + \eta [En_L(r, r') - (2\hbar^2/3m)p_L(r, r')]. \quad (\text{B3}) \end{aligned}$$

The coefficients β , γ , δ , and η are also tabulated in Table I.

We list below the component functions of the kernel. The function $N_L(x)$ which appears is essentially the spherical Bessel function of order L with imaginary argument:

$$N_L(x) = i^L x j_L(ix). \quad (\text{B4})$$

Primes designate differentiations with respect to the argument x .

$$\begin{aligned} U(r) & = 3^8 \mu^{3/2} 2^{-1} (9\mu + \lambda)^{-3/2} \exp(-\gamma_U r^2), \\ \gamma_U & = 9\mu\lambda(9\mu + \lambda)^{-1}. \end{aligned} \quad (\text{B5a})$$

$$\begin{aligned} q_L(r, r') & = 3^{9/2} \mu^2 \pi^{-1/2} (3\mu + \lambda)^{-1} (12\mu + \lambda)^{-1/2} \\ & \quad \times N_L(k_q r r') \exp[-(\gamma_q r^2 + \epsilon_q r'^2)], \quad (\text{B5b}) \end{aligned}$$

$$\begin{aligned} k_q & = (27/2)\mu(3\mu + \lambda)(12\mu + \lambda)^{-1}, \\ \gamma_q & = (9/4)\mu(15\mu + 8\lambda)(12\mu + \lambda)^{-1}, \\ \epsilon_q & = (9/4)\mu(15\mu + 2\lambda)(12\mu + \lambda)^{-1}. \end{aligned}$$

$$s_L(r, r') = q_L(r', r).$$

$$\begin{aligned} t_L(r, r') & = 3^4 \mu^{3/2} 2^{-2} \pi^{-1/2} (3\mu - \lambda)^{-1} N_L(k_t r r') \\ & \quad \times \exp[-\gamma_t(r^2 + r'^2)], \quad (\text{B5c}) \end{aligned}$$

$$\begin{aligned} k_t & = (9/8)(3\mu - \lambda), \\ \gamma_t & = (9/16)(5\mu + \lambda). \end{aligned}$$

$$\begin{aligned} r_L(r, r') & = 3^{9/2} \mu^2 2^{-2} \pi^{-1/2} (3\mu + \lambda)^{-3/2} N_L(k_r r r') \\ & \quad \times \exp[-\gamma_r(r^2 + r'^2)], \quad (\text{B5d}) \end{aligned}$$

$$\begin{aligned} k_r & = 27\mu/8, \\ \gamma_r & = 45\mu/16. \end{aligned}$$

$$\begin{aligned} n_L(r, r') & = -3^3 \mu^{1/2} 2^{-1} \pi^{-1/2} N_L(k_n r r') \\ & \quad \times \exp[-\gamma_n(r^2 + r'^2)]. \quad (\text{B5e}) \end{aligned}$$

$$\begin{aligned} p_L(r, r') & = 3^8 \mu^{3/2} 2^{-7} \pi^{-1/2} \\ & \quad \times \{ [-152/27 + 9\mu(r^2 + r'^2)] \\ & \quad \times N_L(k_p r r') - 14\mu r r' N_L'(k_p r r') \} \\ & \quad \times \exp[-\gamma_p(r^2 + r'^2)]. \quad (\text{B5f}) \end{aligned}$$